catalysts

MDPI

Review

Cofactor F_{420}-Dependent Enzymes: An Under-Explored Resource for Asymmetric Redox Biocatalysis

Mihir V. Shah [1,†], James Antoney [1,2,†], Suk Woo Kang [1,2], Andrew C. Warden [1], Carol J. Hartley [1], Hadi Nazem-Bokaee [1], Colin J. Jackson [1,2] and Colin Scott [1,*]

1 CSIRO Synthetic Biology Future Science Platform, Canberra 2601, Australia; Mihir.Shah@csiro.au (M.V.S.); James.Antoney@anu.edu.au (J.A.); Suk.Kang@anu.edu.au (S.W.K.); andrew.warden@csiro.au (A.C.W.); Carol.Hartley@csiro.au (C.J.H.); Hadi.Nazem-Bokaee@csiro.au (H.N.-B.); colin.jackson@anu.edu.au (C.J.J.)

2 Research School of Chemistry, Australian National University, Canberra 2601, Australia

* Correspondence: colin.scott@csiro.au; Tel.: +61-2-6246-4090

† M.V.S. and J.A. contributed equally to this review.

Received: 20 September 2019; Accepted: 10 October 2019; Published: 20 October 2019

Abstract: The asymmetric reduction of enoates, imines and ketones are among the most important reactions in biocatalysis. These reactions are routinely conducted using enzymes that use nicotinamide cofactors as reductants. The deazaflavin cofactor F_{420} also has electrochemical properties that make it suitable as an alternative to nicotinamide cofactors for use in asymmetric reduction reactions. However, cofactor F_{420}-dependent enzymes remain under-explored as a resource for biocatalysis. This review considers the cofactor F_{420}-dependent enzyme families with the greatest potential for the discovery of new biocatalysts: the flavin/deazaflavin-dependent oxidoreductases (FDORs) and the luciferase-like hydride transferases (LLHTs). The characterized F_{420}-dependent reductions that have the potential for adaptation for biocatalysis are discussed, and the enzymes best suited for use in the reduction of oxidized cofactor F_{420} to allow cofactor recycling in situ are considered. Further discussed are the recent advances in the production of cofactor F_{420} and its functional analog F_O-5′-phosphate, which remains an impediment to the adoption of this family of enzymes for industrial biocatalytic processes. Finally, the prospects for the use of this cofactor and dependent enzymes as a resource for industrial biocatalysis are discussed.

Keywords: cofactor F_{420}; deazaflavin; oxidoreductase; hydride transfer; hydrogenation; asymmetric synthesis; cofactor biosynthesis

1. Introduction

Enzymes that catalyze the asymmetric reduction of activated double bonds are among the most important in biocatalysis, allowing access to chiral amines from imines (C=N), *sec*-alcohols from ketones C=O), and enantiopure products derived from enoates (C=C). To date, the reduction of imines, ketones and enoates has been achieved largely using enzymes that draw their reducing potential from the nicotinamide cofactors NADH and NADPH; e.g., imine reductases, ketoreductases and Old Yellow Enzymes [1–4]. However, there has been recent interest in an alternative reductive cofactor, cofactor F_{420} (8-hydroxy-5-deazaflavin) [5,6].

Cofactor F_{420} is a deazaflavin that is structurally similar to flavins (Figure 1), with a notable difference at position 5 of the isoalloxazine ring, which is a nitrogen in flavins and a carbon in deazaflavins. Additionally, while C-7 and C-8 are methylated in riboflavin, they are not in cofactor F_{420}: C-7 is hydroxylated and C-8 is unsubstituted. These structural differences cause significant differences in the electrochemical properties of cofactor F_{420} and flavins: a −360–340 mV the redox mid-point

potential of cofactor F_{420} is not only lower than that of the flavins (−205 mV to −220 mV), but it is also lower than that of the nicotinamides (−320 mV) [7]. Additionally, as a consequence of the substitution of N-5 for a carbon, cofactor F_{420} cannot form a semiquinone (Figure 1), which means that unlike other flavins, cofactor F_{420} can only perform two-electron reductions.

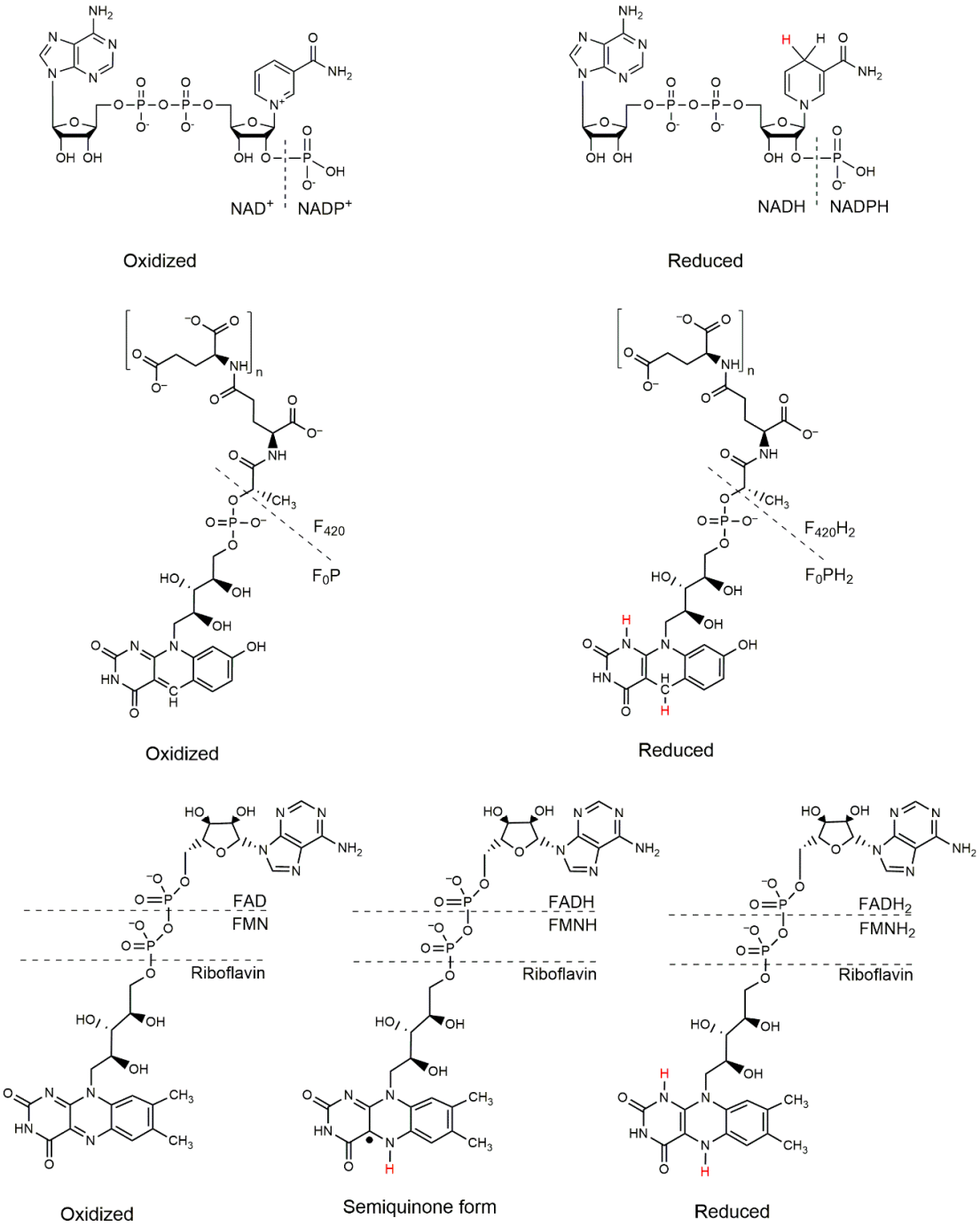

Figure 1. The structures of NAD(P) (top), cofactor F_{420} and its synthetic analog F_OP (center) and common flavins (riboflavin, FMN and FAD; bottom). The oxidized and reduced forms are shown, as is the flavin semiquinone. Dashed lines indicate the differences in the structures of F_OP and cofactor F_{420}, and riboflavin, FMN and FAD.

Cofactor F_{420} was originally described in methanogenic archaea, where it plays a pivotal role in methanogenesis [8,9]. Cofactor F_{420} has since been described in a range of soil bacteria supporting

a range of metabolic activities, including catabolism of recalcitrant molecules (such as picric acid) and the production of secondary metabolites, such as antibiotics [7]. A comprehensive review of the biochemistry and physiological roles of cofactor F_{420} was recently published by Greening and coworkers [7]. This review considers the potential of F_{420}-dependent enzymes in industrial biocatalysis, focusing on the enzyme families relevant to biocatalytic applications and the reactions that they catalysis. Cofactor recycling strategies and cofactor production are also discussed, with a focus on the prospects for achieving low-cost production at scale in the latter case.

2. Families of F_{420}-Dependent Enzymes Relevant to Biocatalysis

With respect to their prospective biocatalytic applications, the two most important families of F_{420}-dependent enzymes are the Flavin/Deazaflavin Oxidoreductase (FDOR) and Luciferase-Like Hydride Transferase (LLHT) families, albeit F_{420}-dependent enzyme from other families have also been shown to have catalytic activities of interest (e.g., TomJ, the imine reducing flavin-dependent monooxygenase or OxyR, the tetracycline oxidoreductase) [10,11]. The FDOR and LLHT families are large and contain highly diverse flavin/deazaflavin-dependent enzymes. In both families, there are enzymes with preferences for flavins, such as flavin mononucleotide (FMN) and flavin adenine dinucleotide (FAD), as well as those that use cofactor F_{420} [12,13]. Moreover, there are F_{420}-dependent FDORs that have been shown to be able to promiscuously bind FMN and use it in oxidation reactions [14]. In this section, the FDOR and LLHT families and the classes of reaction that they catalyze are discussed.

2.1. The FDOR Superfamily

The FDOR superfamily (PFAM Clan CL0336) can be broadly divided into two groups: the FDOR-As (which includes a sub-group called the FDOR-AAs) and the FDOR-Bs. The FDOR-As are restricted to *Actinobacteria* and *Chloroflexi* and to date no FDOR-As have been described that use cofactors other than F_{420} [7,12]. The FDOR-Bs are found in a broader range of bacterial genera than the FDOR-A enzymes, and in addition to F_{420}-dependent enzymes, this group also includes heme oxygenases, flavin-sequestering proteins, pyridoxine 5′ oxidases and a number of proteins of unknown function [12,15–17]. Both groups of FDOR are highly diverse, with many homologs often found within a single bacterial genome (e.g., *Mycobacterium smegmatis* has 28 FDORs) [18]. In addition, the majority of the enzymes of this family are yet to be characterized with respect to either their biochemical or physiological function, and therefore the FDORs represent a currently under-explored source of enzymes for biocatalysis.

The FDOR enzymes share a characteristic split β-barrel fold that forms part of the cofactor-binding pocket. The majority of the protein sequences of enzymes currently identified as belonging to this family are small single-domain proteins. The topologies of the two FDOR subgroups are broadly similar (Figure 2), with the split-barrel core composed of 7–8 strands and with 4–5 helices interspersed. All FDOR-Bs studied so far have been demonstrated to be dimeric, with stands β2, β3, β5 and β6 making up the core of the dimer interface (Figure 2). In structures of full-length FDOR-As solved to date, the N-terminal helix (if present) lies on the opposite face of the beta sheet to that in FDOR-Bs. Thus, the N-terminus occupies part of the dimer interface region and prevents interaction between the sheets of adjacent monomers. In contrast to the FDOR-Bs, the oligomerization state of the FDOR-As is more varied. While a number of FDOR-As have been determined to be monomeric [18], the deazaflavin-dependent nitroreductase (DDN) from *M. tuberculosis* forms soluble aggregates through the amphipathic N-terminal helix [19]. DDN and the FDOR-AA subgroup have been shown to be membrane-associated [20–22], and FDOR-AAs have been associated with fatty acid metabolism [12]. No structures of FDOR-AAs have been solved to date.

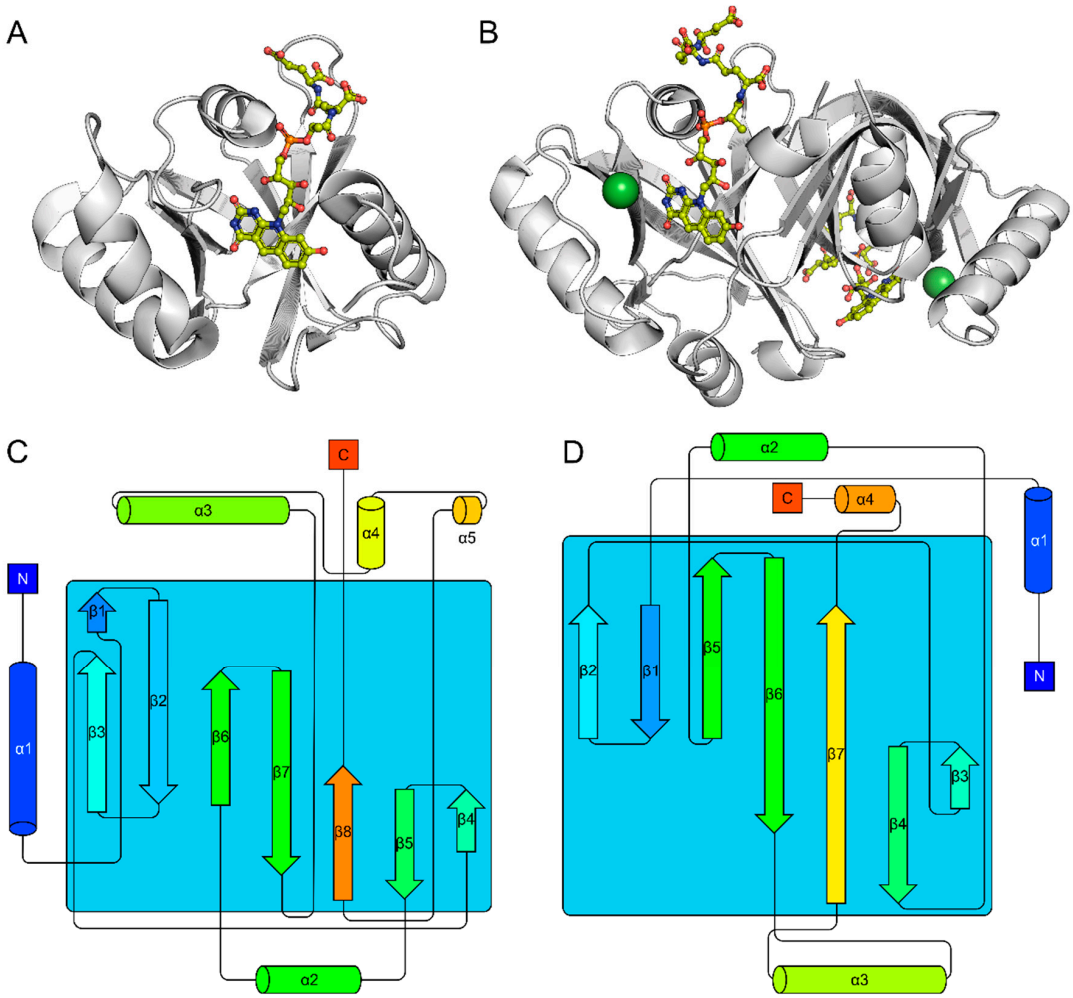

Figure 2. Representative structures of F_{420}-dependent FDOR-A (PDB: 3R5Z, panels **A** and **C**) and FDOR-B (PDB: 5JAB, panels **B** and **D**). Both are predominantly composed of a single β-sheet forming a split barrel. The N-terminal helices are spatially displaced between the two families, falling on opposite faces of the β-sheet.

2.2. The LLHT Family:

The LLHT family form part of the Luciferase-Like Monooxygenase family (PFAM PF00296). They adopt an $(\alpha/\beta)_8$ TIM-barrel fold with three insertion regions, IS1–4 (Figure 3). IS1 contains a short loop and forms part of the substrate cleft. IS2 contains two antiparallel β-strands, and IS3 contains a helical bundle at the C-terminus of the β-barrel and contains the remainder of the substrate-binding pocket (Figure 3). All structures solved to date from the LLHT family contain a non-prolyl *cis* peptide in β3 [23–26]. Recent phylogenetic reconstructions have shown that the F_{420}-dependent LLHTs form two clades: the F_{420}-dependent reductases and the F_{420}-depented dehydrogenases [27]. The F_{420}-reductases contain methylenetetrahydromethanopterin reductases (MERs), which catalyze the reversable, ring-opening cleavage of a carbon-nitrogen bond during the biosynthesis of folate in some archaea [28–30]. The F_{420}-dependent dehydrogenases can be further divided into three subgroups. The first contains F_{420}-dependent secondary alcohol dehydrogenases (ADFs) and the hydroxymycolic acid reductase from *M. tuberculosis* [31]. The second contains the F_{420}-dependent glucose-6-phosphate dehydrogenases (FGDs) from *Mycobacteria* and *Rhodococcus*, while the third appear to be more general sugar-phosphate dehydrogenases [27]. In contrast to the heterodimeric structure of bacterial luciferase, the F_{420}-dependent dehydrogenases form homodimers with the dimer interface burying a relatively large portion of the surface area of the monomers (≈2000 $Å^2$, roughly 15%

of the total surface area) [24–26]. A number of enzymes involved in the F_{420}-dependent degradation of nitroaromatic explosives, such as picrate and 2,4-dinitroanisole, appear to belong to the LLHT family as well [32,33].

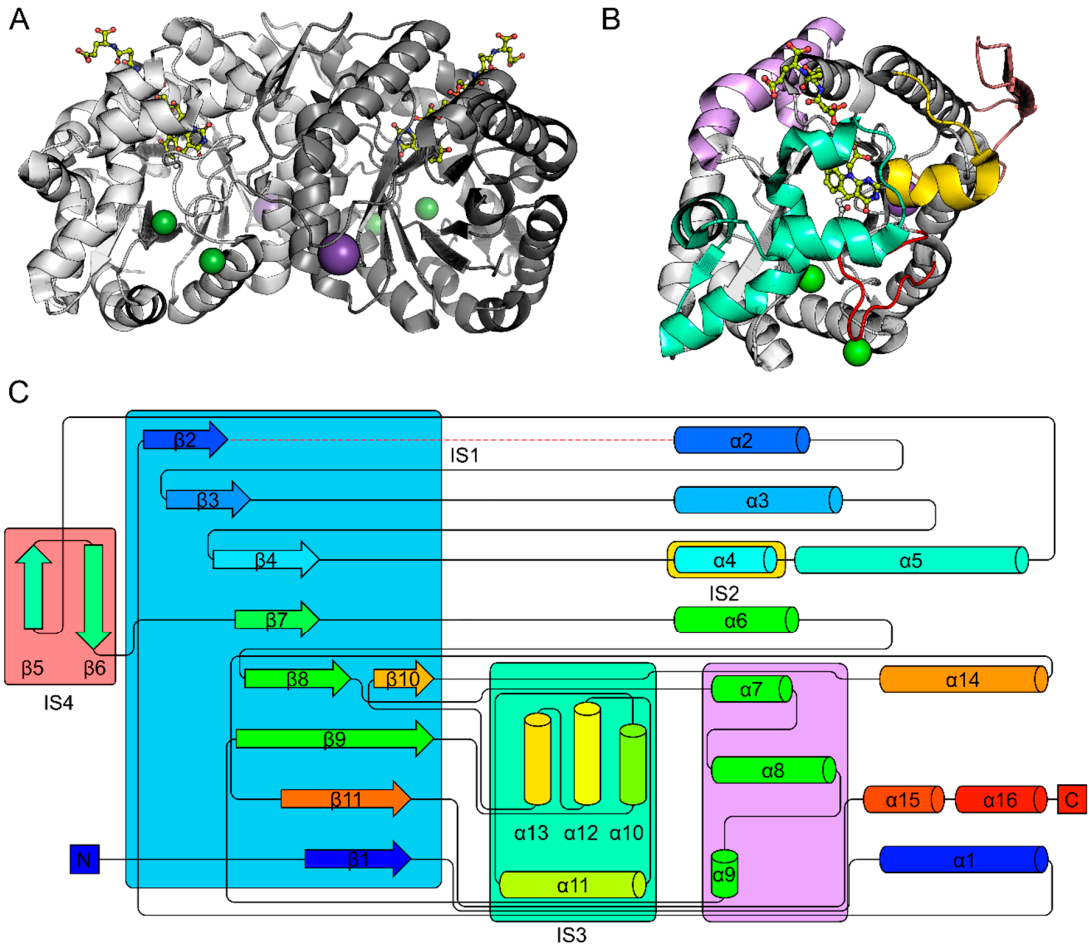

Figure 3. Structure of representative luciferase-like hydride transferase (LLHT) (PDB: 1RHC). (**A**) A 3D representation of the biologically relevant dimer (panel **A**). Monomer of an LLHT with insertion sequences IS1–4 highlighted, along with the helical bundle composed of α7–9 (panel **B**). Topology diagram showing $(\alpha/\beta)_8$ fold with insertion sequences highlighted: IS1, red; IS2, orange; IS3, light green, IS4, pink. The helical bundle of α7–9 is highlighted in purple (panel **C**).

2.3. *Cofactor F_{420}-Dependent Reactions with Relevance to Biocatalysis*

From the perspective of biocatalysis, cofactor F_{420}-dependent enzymes catalyze a number of key reductions including the reduction of enoates, imines, ketones and nitro-groups (Table 1; Figure 4).

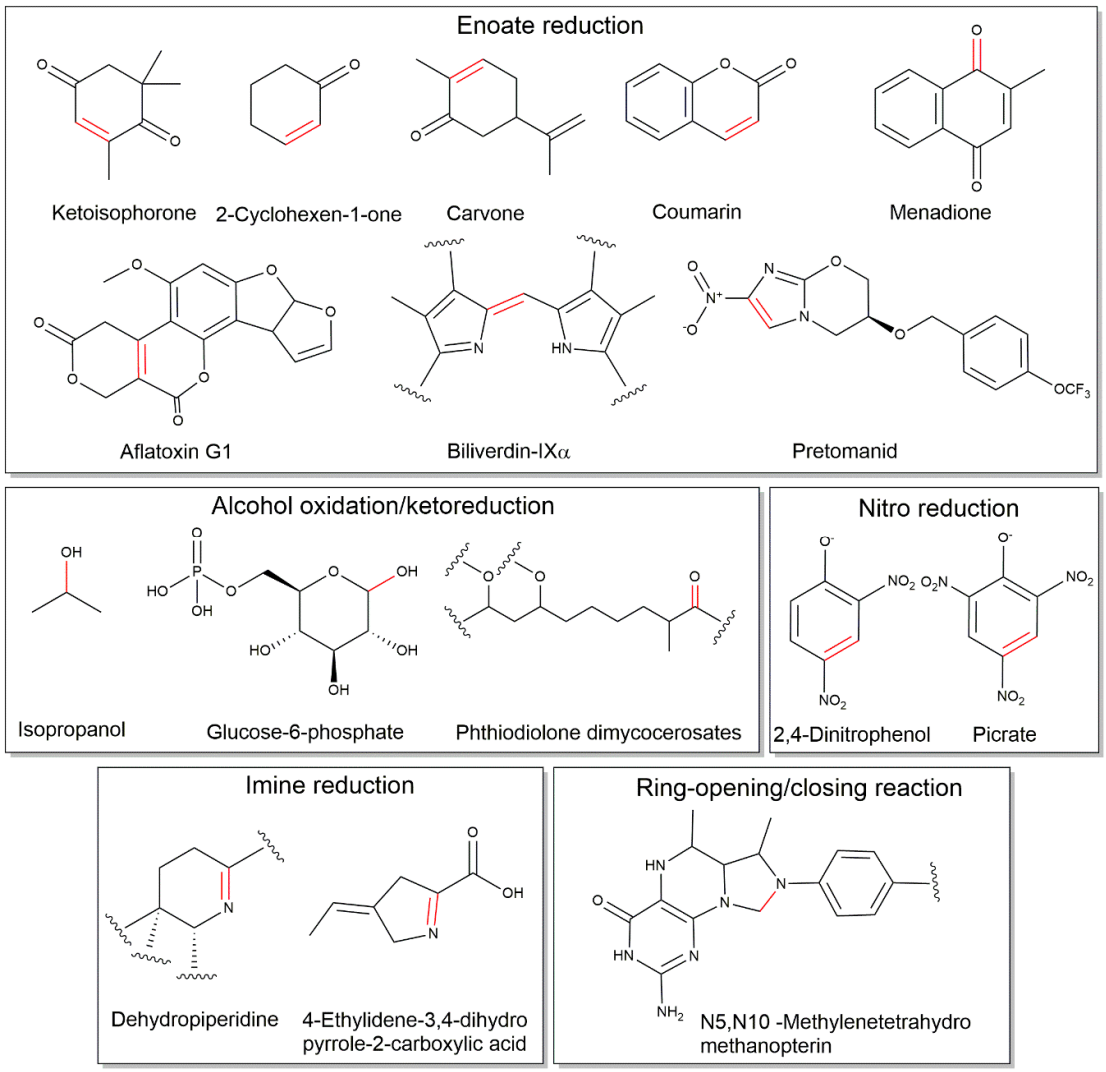

Figure 4. Representative cofactor F_{420}-dependent oxidoreductions with the potential for adaptation to biocatalytic applications. Included are: nitroreduction, enoate reduction, ketoreduction and imine reduction (from top to bottom). For clarity, only the dehydropiperidine ring of the thiopeptide is shown and partial structures for biliverdin-Ixα and phthiodiolone dimycocerosates are shown.

For enoate reductions, a small number of FDORs have been studied. However, the substrate range for most of these enzymes is yet to be fully elucidated. The ability of the mycobacterial FDORs to reduce activated C=C double bonds was first identified when DDN was shown to be responsible for activating the bicyclic nitroimidazole PA-824 in *M. tuberculosis*. These enzymes were then shown to also reduce enoates in aflatoxins, coumarins, furanocoumarins and quinones [6,12,14,16,34–38]. Recent studies have shown that these enzymes are promiscuous and can use cyclohexen-1-one, malachite green and a wide range of other activated ene compounds as substrates [35]. However, there have been a few FDOR studies to date that have examined their kinetic properties and stereospecificity. In one of these studies, FDORs from *Mycobacterium hassiacum* (FDR-Mha) and *Rhodococcus jostii* RHA1 (FDR-Rh1 and FDR-Rh2) were shown to reduce a range of structurally diverse enoates with conversions ranging from 12 to >99% and *e.e.* values of up to >99% [6]. Interestingly, it has been proposed that both the hydride and proton transfer from $F_{420}H_2$ in these reactions was directed to the same face of the activated double bond (Figure 5), which results in the opposite enantioselectivity compared to that of the FMN-dependent Old Yellow Enzyme family of enoate reductases [6]. This suggests that the F_{420}-dependent FDORs may provide a stereocomplementary enoate reductase toolbox. However, other studies suggest that protonation of the substrate is mediated by solvent or an enzyme side-chain (as it

is in Old Yellow Enzyme) [37]. Further structure/function studies are needed to fully understand the mechanistic diversity of this family of enzymes.

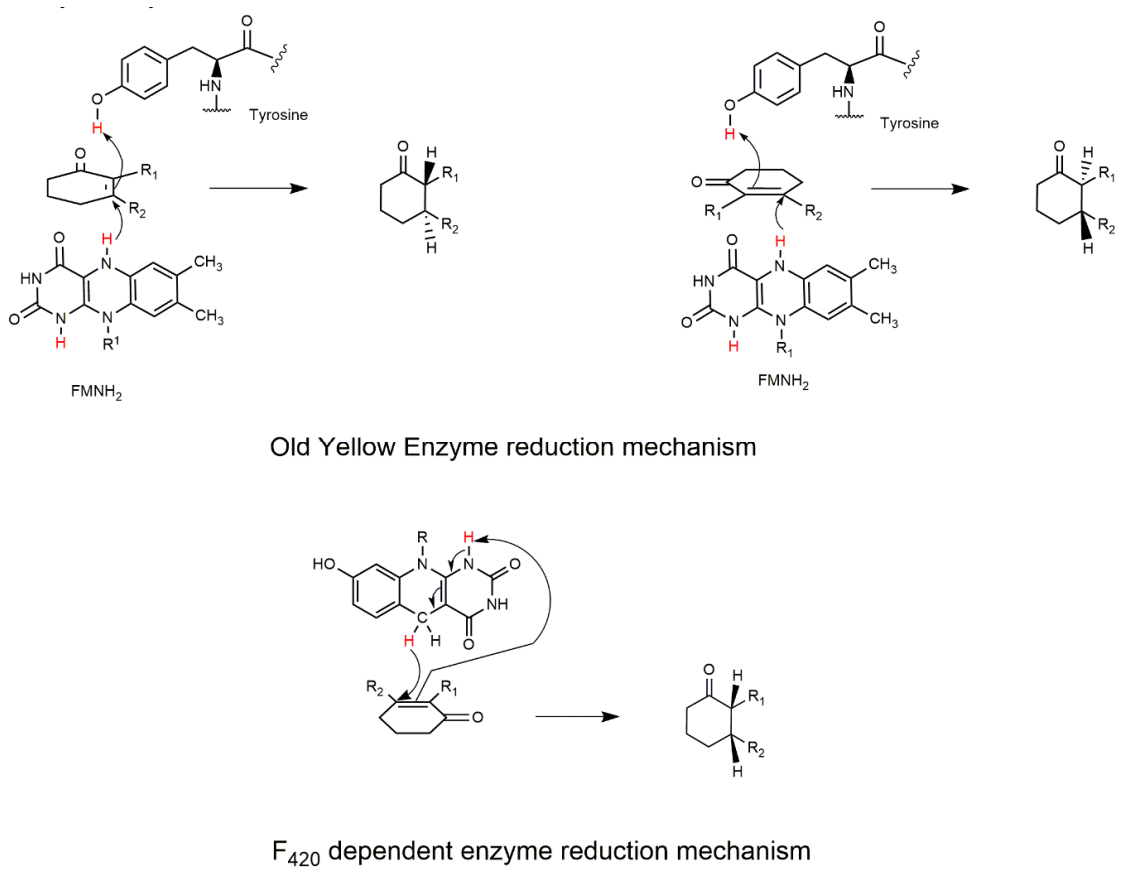

Figure 5. Enoate reduction by a flavin-dependent enzyme (Old Yellow Enzyme) and the proposed mechanism for cofactor F_{420}-dependent reduction. Notably the mechanism of reduction yields *trans*-hydrogenation products for Old Yellow Enzyme and *cis*-hydrogenation products for the F_{420}-dependent enzymes.

The LLHT family contains several enzymes with alcohol oxidase or ketoreductase activity (Table 1; Figure 4). The F_{420}-dependent glucose-6-phosphate dehydrogenases of several species have been investigated [25,26,39]. Although an extensive survey of their substrate ranges has yet to be conducted, it has been demonstrated that glucose is a substrate for the *Rhodococcus jostii* RHA1 enzymes [26]. An F_{420}-dependent alcohol dehydrogenase (ADH) from *Methanogenium liminatans* has been shown to catalyze the oxidation of the short chain aliphatic alcohols 2-propanol, 2-butanol and 2-pentanol (85, 49 and 23.1 s^{-1} k_{cat}, 2.2, 1.2 and 7.2 mM K_M respectively) [40], but it was unable to oxidize primary alcohols, polyols or secondary alcohols with more than five carbons. It is unclear whether these alcohol oxidations are reversible, but in the oxidative direction, these reactions provide enzymes that can be used to recycle reduced cofactor F_{420} (see Section 4). Alcohol oxidation can also be used to produce ketones as intermediates in biocatalytic cascades that can then be used in subsequent reactions, such those catalyzed by transaminases or amine dehydrogenases in chiral amine synthesis [1,41–43] or by ketoreductases or alcohol dehydrogenases in chiral *sec*-alcohol synthesis (i.e., deracemization or stereoinversion of *sec*-alcohols). This approach can be achieved in a one pot cascade if different cofactors are used for the oxidation and reduction (Figure 6) [44].

At least one F_{420}-dependent ketoreductase has been described. The mycobacterial F_{420}-dependent phthiodiolone ketoreductase catalyzes a key reduction in the production of phthiocerol dimycocerosate, a diacylated polyketide found in the mycobacterial cell wall [45]. Although the physiological role of

this enzyme has been elucidated, biochemical studies of the catalytic properties and substrate range are required to assess this enzymes' potential for use as a biocatalyst.

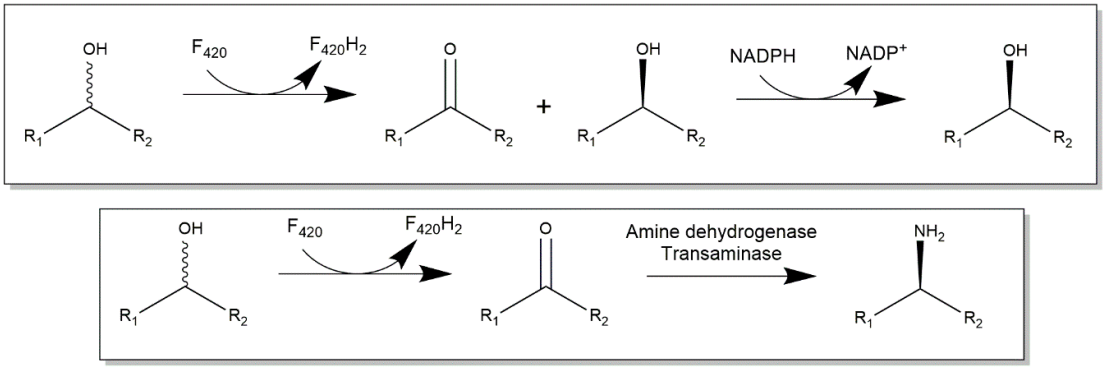

Figure 6. Proposed scheme for one-pot, enzyme cascades for deracemization/steroinversion of *sec*-alcohols (top) and chiral amine synthesis (bottom) using cofactor F_{420}-dependent alcohol oxidation.

F_{420}-dependent enzymes have also been shown to reduce imines (Table 1; Figure 4). An FDOR fromr *Streptomyces tateyamensis* (TpnL) is responsible for the reduction of dehydropiperidine in the piperidine-containing series *a* group of thiopeptide antibiotics produced in this bacterium (Figure 4). TpnL was identified as the F_{420}-dependent dehydropiperidine reductase responsible for the reduction of dehydropiperidine ring in thiostrepton A to produce the piperidine ring in the core macrocycle of thiostrepton A [45]. TpnL activity was affected by substrate inhibition at concentrations higher than 2 μM of thiostrepton A, preventing the measurement of the K_M, but its k_{cat}/K_M was measured at 2.80×10^4 M^{-1} S^{-1} [45]. The substrates for phthiodiolone ketoreductase and TpnL are large secondary metabolites and, as yet, it is unclear if it will accept smaller substrates or substrates with larger/smaller heterocycles (e.g., dehydropyrroles).

Another F_{420}-dependent imine reductase (TomJ) has been described from *Streptomyces achromogenes* that reduces the imine in 4-ethylidene-3,4-dehydropyrrole-2-carboxylic acid during the production of the secondary metabolite tomaymycin, which has been shown to have potentially interesting pharmaceutical properties [11]. Additionally, the reduction of a prochiral dihydropyrrole to a pyrrole is a reaction with a number of biocatalytic applications [5].

Nitroreductases have the potential application in the reduction of a prochiral nitro group to form a chiral amine [46]. The LLHT family F_{420}-dependent nitroreductase Npd from *Rhodococcus* catalyzes the two-electron reduction of two nitro groups in picric acid during catabolism of the explosive TNT (Table 1; Figure 4) [47]. While this stops short of reducing the nitro group to an amine, this catalytic activity may contribute to a reductive cascade that achieves this conversion.

The final class of reaction for consideration in this review is the unusual, reversable ring-opening/closing reaction catalyzed by the MERs (Figure 4; Table 1). This reaction is required for folate biosynthesis in some archaea [23,28–30]. However, ring-closing reactions of this type could be used for producing N-containing heterocycles, which are intermediates in the synthesis of numerous pharmaceuticals [48,49]. The promiscuity of the MERs has not yet been investigated, and so the potential to re-engineer these enzymes is not fully understood.

Table 1. Characterized F_{420}-dependent enzymes with activities that could be adapted for biocatalytic applications.

Reaction	Family	Reference
Enoate reduction		
Aflatoxins	FDOR	[14,18,34]
Coumarins	FDOR	[14,34,35]
Quinones	FDOR	[36]
Biliverdin reduction	FDOR	[12,16]
Nitroimidazoles	FDOR	[36]
Cyclohexenones	FDOR	[6,34,38]
Citral/Neral/Geranial	FDOR	[6]
Carvone	FDOR	[6]
Ketoisophorone	FDOR	[6]
Alcohol oxidation/ketoreduction		
Glucose-6-phosphate	LLHT	[26,50]
Phthiodiolone dimycocerosate	LLHT	[51]
Isopropanol	LLHT	[40]
Imine reductions		
Dehydropiperidine (in thiopeptins)	FDOR	[45]
4-ethylidene-3,4-dihydropyrrole-2-carboxylic acid	Flavin-dependent monooxygenase	[11]
Nitroreductions		
Picrate	LLHT	[47,50]
2,4-DNP	LLHT	[48,50]
Ring opening/closing		
C-N bond cleavage/formation in methylenetetrahydromethanopterin	LLHT	[23,28–30]

3. Cofactor Recycling for Cofactor F_{420}

Cofactor recycling is essential for the practical application of the F_{420}-dependent enzymatic processes in biocatalysis. There are various strategies for cofactor regeneration for NADH and NADPH, including enzymatic, chemical, electrochemical and photochemical methods [52]. In this section, the potential enzymes for the regeneration of cofactor F_{420} are discussed. As most of the industrially relevant F_{420}-dependent reactions are asymmetric reductions, F_{420}-dependent oxidases are required for cofactor regeneration. Figure 7 shows the characterized enzymes that catalyze F_{420}-dependent oxidations that could be applied in cofactor F_{420} reduction.

Emulating methods developed for nicotinamide cofactors, both formate dehydrogenase (FDH) and glucose 6-phosphate dehydrogenase (G6PD) enzymes are attractive enzymatic routes for cofactor reduction both in vitro [53–56] and in vivo [57,58]. Fortunately, F_{420}-dependent G6PDs and FDHs have been identified and characterized. The F_{420}-dependent G6PD from *Mycobacteria* (FGD) is one potential cofactor F_{420}-recycling enzyme. FGD is the only enzyme in these bacteria known to reduce oxidized cofactor F_{420}. The intracellular concentration of G6P in *Mycobacteria* is up to 100-fold higher than it is in *E. coli*, which provides a ready source of reducing power for F_{420}-dependent reduction reactions [59]. FGD from *Rhodococcus jostii* and *Mycobacterium smegmatis* have been studied and expressed in *E. coli*, both the enzymes were stable in in vitro assays [26,39,60]. Both FGDs have been expressed in engineered *E. coli* producing cofactor F_{420} together with FDORs [38,59] FGDs have been shown to efficiently regenerate reduced cofactor F_{420} both in vivo and in vitro. However, the cost of the glucose-6-phosphate and the need to separate reaction products from the accumulated FGD byproduct (6-phosphoglucono-D-lactone) may prove to be impediments for the adoption of FGD as a recycling system for cofactor F_{420} in the in vitro biotransformations.

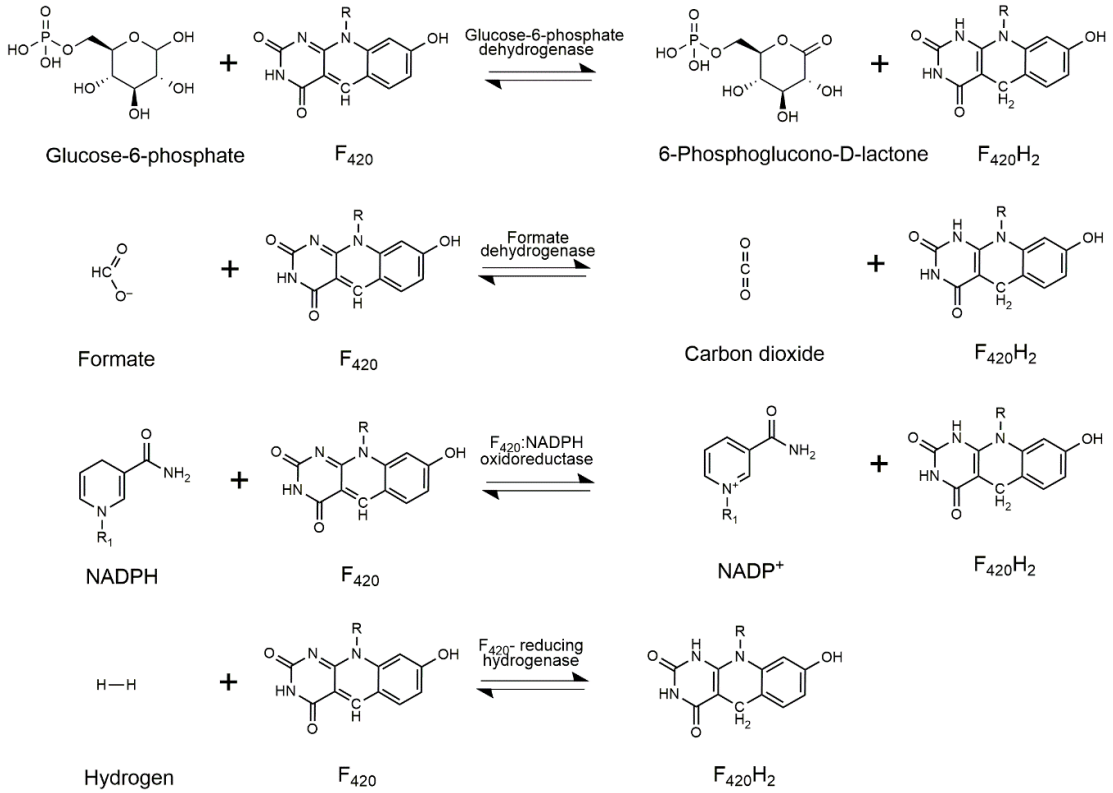

Figure 7. Cofactor F_{420}-dependent oxidation reactions that could be exploited to produce reduced cofactor F_{420}.

Formate is an excellent reductant for cofactor recycling, with FDH-dependent cofactor reduction yielding carbon dioxide, a volatile byproduct that can be easily removed from the reaction mixture, thereby simplifying the downstream processing of the product of interest. Additionally, formate is a low-cost reagent, leading to favorable process economics. Most methanogens have the capability to use formate as sole electron donor using F_{420}-dependent formate dehydrogenase [61]. The soluble F_{420}-dependent FDH from *Methanobacterium formicium* has been expressed in *E. coli* [62], purified and studied in vitro with the reduction of 41.2 μmol of F_{420} min^{-1} mg^{-1} of FDH, with non-covalently bound FAD required for optimal activity [8]. *Methanobacterium ruminantium* FDH reduces cofactor F_{420} at a much slower rate than *M. formicium*: 0.11 μmol of F_{420} min^{-1} mg^{-1} of FDH [8]. As yet, the use of F_{420}-dependnt FDHs for in vitro cofactor recycling has been sparsely studied. However, as these enzymes are soluble and can be heterologously expressed, they represent a promising system for use in cofactor F_{420}-dependent biocatalytic processes.

Another potential recycling system for cofactor F_{420} is the F_{420}:NADPH oxidoreductase (Fno), which couples the reduction of cofactor F_{420} with oxidation of NADPH. Methanogenic archaea use this enzyme to transfer reducing equivalents from hydrogenases to produce NADPH via F_{420}, while in bacteria it functions in the opposite direction, that is, to provide the cell with reduced F_{420} via NADPH [63]. Fno is also required for the production of reduced F_{420} for tetracycline production in *Streptomyces* [63]. The Fno enzymes from the thermophilic bacteria *Thermobifida fusca* and the thermophilic archaeon *Archeoglobus fulgidus* have been expressed in *E. coli* [64,65]. These enzymes are thermostable, with their highest activity observed at 65 °C. As the redox midpoint potentials of NADP and cofactor F_{420} are very similar, it is perhaps unsurprising that pH has a significant influence on the equilibrium of the reaction, with the reduction of $NADP^+$ favored at high pH (8–10) and the reduction of F_{420} favored at low pH (4–6) [64,65]. The Fno *Streptomyces griseus* has also been purified and characterized, and also displayed pH-dependent reaction directionality [66]. Fno may be an excellent enzyme for the in vivo reduction of cofactor $F_{420,}$ where NADPH would be provided from

central metabolism. However, for its use as a cofactor F_{420} recycling enzyme in vitro, Fno would need to be coupled with an NADPH regenerating enzyme, such as an NADPH-dependent formate dehydrogenase [67]. This added complexity and cost may limit the use of Fno-dependent cofactor F_{420} recycling in vivo.

Hydrogenotrophic archaea, including methanogens and sulfate-reducing archaea, possess an essential, cofactor F_{420}-dependent hydrogenase (FhrAGB) [68–71]. These nickel/iron enzymes could potentially be used in vivo to allow the direct H_2-dependent reduction of cofactor F_{420}. However, as these heterododecameric enzymes have complex cofactor requirements (four [4Fe 4S] clusters, and NiFe center and FAD), are oxygen-sensitive and tend to aggregate [71], it is unclear if they can be made suitable for in vitro use.

4. Cofactor Production

The lack of a scalable production system for cofactor F_{420} has been noted as a major impediment to the adoption of F_{420}-dependent enzymes by industry [5]. Cofactor F_{420} is available as a research reagent (http://www.gecco-biotech.com/), but its production at scale is not yet economic. In fact, most research laboratories with an interest in cofactor F_{420}-dependent enzymes synthesize and purify the cofactor themselves using slow-growing F_{420} producing microorganisms, most commonly methanogens and actinobacteria (Table 2). The economic production of cofactor F_{420} at large scale is not feasible using natural producers as they are ill-suited to industrial fermentation and generally lack the genetic tools required to improve cofactor F_{420} yield.

Table 2. Published production systems for cofactor F_{420}.

Source	F_{420} Yield (µmol/g Cell Weight)	Growth Conditions	Ref
Methanobacterium thermoautotrophicum	0.42 [a,c]	Grown at 60 °C using complex media in fermenter, under pressurized hydrogen	[9]
Methanobacterium formicium	0.27 [a,c]	Grown at 37 °C using complex media in fermenters	[9]
Methanospirillum hungatii	0.41 [a,c]	Grown at 37 °C using complex media in fermenters	[9]
Methanobacterium strain M.o.H	0.53 [a,c]	Grown at 40 °C using complex media in fermenters	[9]
Methanobacterium thermoautotrophicum	1.7 [e]	Grown using complex media in fermenters, under pressurized hydrogen gas	[73]
Streptomyces flocculus	0.62 [e]	Grown using complex media in fermenters	[73]
Streptomyces coelicolor	0.04 [e]	Grown using complex media in fermenters	[73]
Streptomyces griseus	0.008 [a,c]	Growth conditions not mentioned in the publication	[74]
Rhodococcus rhodochrous	0.11 [e]	Grown using complex media in fermenters	[73]
Mycobacterium smegmatis	0.30 [e]	Grown using complex media in fermenters	[73]
Mycobacterium smegmatis	3.0 [d]	Overexpression of F_{420} pathway genes, cultivation in complex media at 37 °C in shake flasks	[72]
Escherichia coli	0.38 [b]	Overexpressing F_{420} pathway genes, grown in minimal media at 30 °C in shake flasks.	[59]

[a] Mol weight of F_{420} with 1 glutamate tail is 773.6 Da, which was used to convert values published as µg of F_{420}, noting that micro-organisms produce mixture of F_{420} with different number of glutamates (1–9) attached. [b] Concentration estimated through absorbance at 420 nm and using extinction coefficient of 41.4 mM^{-1} cm^{-1} [73]. [c] F_{420} concentration per g of wet cell weight. [d] Concentration of F_{420} not mentioned in the publication, but F_{420} yield was stated to be 10 times higher than wild-type *M. smegmatis*. [e] Concentration estimated through absorbance at 400 nm and using extinction coefficient of 25.7 mM^{-1} cm^{-1} [74].

Recently, there have been significant advances towards the scalable production of the cofactor for F_{420}-dependent enzymes. *M. smegmatis* has been engineered to overexpress the biosynthetic genes for cofactor F_{420} production, leading to a substantial improvement in yields (Table 2) [72]. However, *M. smegmatis* is not ideally suited as a fermentation organism as it is slow growing, forms clumps

during cultivation and is not recognized as GRAS (generally regarded as safe). More recently, the biosynthetic pathway for cofactor F_{420} has been successfully transplanted to *E. coli* [59], allowing the heterologous production of the cofactor at levels similar to those of the natural F_{420} producers (Table 2) [59], accumulated to 0.38 μmol of F_{420} per gram of dry cells.

There is scope to further improve the production of F_{420} in *E. coli*. Cofactor F_{420} does not appear to be toxic to *E. coli* [59], which suggests that there is little interaction between F_{420} and the enzymes *E. coli* (although this is yet to be confirmed experimentally). The thermodynamics of cofactor F_{420} production are favorable (Appendix A), suggesting that there are no major thermodynamic impediments to improving yield. Interestingly, the first dedicated step of cofactor F_{420} production (catalyzed by CofC/FbiD) is not energetically favorable and may consequently be sensitive to intracellular metabolite concentrations. In addition to the engineering considerations that this may impose, it may also be responsible for the biochemical diversity of this step in different microorganisms. In different microbes, the CofC/FbiD-dependent step uses 2-phospholactate [75], 3-phosphoglycerate [76] or phosphoenolpyruvate [59] as a substrate, which may reflect the relative abundance of those metabolites in various bacteria and archaea and the thermodynamic constraints on this step.

Another recent advance is the production of a synthetic analog of cofactor F_{420}, called F_O-5′-phosphate (F_OP). F_OP was derived from F_O, the metabolic precursor of cofactor F_{420}, which is phosphorylated using an engineered riboflavin kinase [38]. F_OP has also been shown to function as an active cofactor for cofactor F_{420}-dependent enzymes activities, albeit there is a penalty in the rates of these reactions [38]. Drenth and coworkers prepared F_O by chemical synthesis, using a method developed by Hossain et al. [77]. However, it is likely that the engineered kinase for the phosphorylation of F_O could be introduced into an organism that over-produces F_O allowing for the production of F_OP by fermentation. This semisynthetic pathway would have the advantage that it needs only two biosynthetic steps, instead of the four steps needed for cofactor F_{420} production, and demands less metabolic input from the native host metabolism (e.g., no glutamate is required) [38]. The production of F_OP also opens the possibility of making deazaflavin analogs of FMN and FAD, which would be electrochemically more like F_{420} than flavins, but may still bind FMN and FAD- dependent enzymes and potentially allow access to new chemistry with already well-characterized enzymes.

5. Prospects

Reduced cofactor F_{420} is electrochemically well suited for biocatalytic applications, and the small number of F_{420}-dependent enzymes characterized to date show promise as potential biocatalysts (as discussed above). However, before these enzymes can be widely and effectively used as biocatalysts, further research is needed to better characterize them as the biochemistry of cofactor F_{420}-dependent enzymes remains under-explored. The LLHT and FDOR families are a rich source of highly diverse enzymes with considerable potential for biocatalysis, albeit much of the research to date has focused on the physiological roles of these enzymes, rather than their in vitro enzymology. Although some of these enzymes have been shown to have small molecule substrates, those involved with secondary metabolite biosynthesis tend to act on high molecular weight substrates and it is not yet clear whether they will accept lower molecular weight molecules.

To be cost competitive, cofactor F_{420} needs to have effective recycling systems. The enzymes for cofactor recycling have already been identified, although there have been a few studies investigating their performance in this role. Moreover, alternative cofactor recycling strategies, such electrochemical or photochemical recycling, have not yet been investigated for cofactor F_{420}. The production of cofactor F_{420} at scale and at low cost remains a roadblock for the use of these enzymes by industry. However, considerable progress has been made on this front in the last few years and it is likely that low cost cofactor F_{420}, or F_{420} surrogates, will soon be available. Additionally, the availability of F_{420}-producing bacteria with tools for facile genetic manipulation, along with a growing number of empirically determined protein structures, opens up the prospect of improving this class of enzymes using in vitro evolution and rational design. It is notable that there is still some uncertainty concerning

the mechanistic detail of F_{420}-dependent reactions, which need to be addressed through a detailed structure/function analysis to enable a rational design of these enzymes.

Supplementary Materials: The following are available online at http://www.mdpi.com/2073-4344/9/10/868/s1.

Author Contributions: Writing—original draft preparation, M.V.S., J.A., S.W.K., H.N.-B., C.J.J. and C.S.; writing—review and editing, M.V.S., J.A., S.W.K., H.N.-B., A.C.W., C.J.H., C.J.J. and C.S.

Funding: M.V.S. and H.N.-B. are funded by the CSIRO Synthetic Biology Future Science Platform. J.A. is funded by the Australian Government Research Training Program (AGRTP) and S.W.K. is funded by the Korean Institute of Science and Technology and the AGRTP.

Conflicts of Interest: The authors declare no conflict of interest.

Abbreviations

5AD: 5′-Deoxyadenosine; 5ARPD: 5-amino-6-(D-ribitylamino)uracil; 5ARPD4HB: 5-amino-5-(4-hydroxybenzyl)-6-(D-ribitylimino)-5,6-dihydrouracil; d_{F420}-0: Dehydro coenzyme F_{420}-0 (oxidized); EPPG: Enolpyruvyl-diphospho-5′-guanosine; F_o: 7,8-Didemethyl-8-hydroxy-5-deazariboflavin; F_{420}-0: Coenzyme F_{420}-0 (oxidized); F_{420}-1: Coenzyme F_{420}-1 (oxidized); F_{420}-2: Coenzyme F_{420}-2 (oxidized); F_{420}-3: Coenzyme F_{420}-3 (oxidized); FMN: Flavin mononucleotide (oxidized); $FMNH_2$: Flavin mononucleotide (reduced); GDP: Guanosine diphosphate; GMP: Guanosine monophosphate; Glu: L-Glutamate; GTP: Guanosine triphosphate; H^+: Proton; ImiAce: 2-iminoacetate or Dehydroglycine; Met: L-Methionine; NH_4: Ammonium; PEP: Phosphoenolpyruvate; Pi: Phosphate; PPi: Diphosphate; SAMe: S-Adenosyl-L-methionine; Tyr: L-Tyrosine.

Appendix A Thermodynamics of F420 Biosynthesis

The thermodynamic properties of each of the steps in cofactor F_{420} biosynthesis were estimated to evaluate the feasibility of increasing the production of the cofactor in an engineered microorganism. The pathway assembled by Bashiri et al. [59] in *E. coli* was used (i.e., PEP was used as substrate for CofC). The standard transformed Gibbs free energy ($\Delta_r G^t$) of each step were calculated under the physiological conditions (25 °C, pH 7, and ionic concentration of 0.25 M) as described elsewhere [78,79]. The overall Gibbs free energy (ΔG^t) was then calculated by summing up all individual $\Delta_r G^t$ (Table A1). The Gibbs free energy of metabolite formation ($\Delta_f G$) for each metabolite in the pathway was obtained (Supplementary Information) from comprehensive lists of metabolites whose $\Delta_f G$ were estimated using a group contribution method [80,81]. The $\Delta_f G$ for each metabolite was then converted into its transformed type ($\Delta_f G^t$) method of Alberty [78]. The data were collected from relevant biochemical databases and the literature for any metabolite with missing $\Delta_f G$ [82–84]. Owing to possessing different protonation states, the inconsistencies in $\Delta_f G$ of certain metabolites such as the glutamates in F_{420}-n among databases and the literature are inevitable. Thus, $\Delta_r G^t$ for reactions containing metabolites with varying $\Delta_f G$ were calculated considering the differences in their $\Delta_f G$ leading to the generation of a total of four sets of $\Delta_r G^t$. Finally, the mean and standard deviations were calculated for these sets to yield the variation in each reaction as well as in the overall pathway (Table A1).

The data shown in Table A1 confirms that the overall cofactor F_{420} biosynthesis pathway is thermodynamically feasible under the given conditions. However, certain steps in this pathway impose a thermodynamic barrier with respect to the physiological conditions examined. For example, CofC seems to be one of the major thermodynamically unfavorable steps in the whole pathway possibly due to the energy-dependent synthesis of EPPG, one of the precursors for making F_{420}. CofG/H combined appears to be the most thermodynamically favorable step in the whole pathway driving the biosynthesis of F_0, the other key precursor for F_{420} biosynthesis. Interestingly, the formation of F_{420}-2 molecule seems to be the most favorable step among other F_{420} molecules downstream of the pathway. It should be noted that the thermodynamic calculations were only performed up to three steps of F_{420} molecule production (i.e., F_{420}-3) largely because of the high levels of inconsistencies of the data available for $\Delta_f G$ of higher F_{420} molecules.

Table A1. Standard transformed Gibbs free energy of reaction (Δ_rG^t), for the F_{420} biosynthesis pathway, calculated based on Gibbs free energy of metabolite formation (Δ_fG^t) calculated at 25 °C, pH of 7, and ionic concentration of 0.25 M.

Enzyme	Reaction [a]	Δ_rG^t (kJ) [b]
CofC/FbiD	PEP + GTP → EPPG + PP_i [d]	+71.27(±67)
CofG/FbiC	5ARPD + Tyr + SAMe → 5ARPD4HB + ImAcet + Met + 5AD	−1192.39(±0) [c]
CofH/FbiC	5ARPD4HB + SAMe → F_O + NH_4^+ + Met + 5AD	+71.90(±36) [c]
CofD/FbiA	F_O + EPPG → d_{F420}-0 + GMP	−31.3(±128)
CofX/FbiB	d_{F420}-0 + $FMNH_2$ → F_{420}-0 + FMN	−74.59(±87)
CofE/FbiB	F_{420}-0 + GTP + Glu → F_{420}-1 + GDP + P_i	−7.50(±24)
CofE/FbiB	F_{420}-1 + GTP + Glu → F_{420}-2 + GDP + P_i	−39.44(±35)
CofE/FbiB	F_{420}-2 + GTP + Glu → F_{420}-3 + GDP + P_i	−21.99(±38)
Overall	PEP + 5ARPD + Tyr + (2) SAMe + $FMNH_2$ + (3) Glu + (4) GTP → F_{420}-3 + (2) Met + (2) 5AD + ImAcet + NH_4^+ + FMN + (3) GDP + (3) P_i + GMP + PP_i	−1224.05(±82)

[a] For simplicity, protons were omitted in these equations and subsequent calculations as the Δ_fG^t of a proton under the set conditions is ~0.08 kJ. However, all Δ_rG^t calculations are based on a balanced equation. [b] The mean values of four sets and their standard deviations in parenthesis shown for each reaction. [c] Δ_fG of 5ARPD4HB has only been reported in MetaCyc inferred by computational analysis. Including it in the calculations of Δ_rG^t for CofG and CofH results in −225.88(±0) and −894.62(±36), respectively. [d] Hydrolysis of PP_i ($H_3P_2O_7^{3-}$ + H_2O → 2 HPO_4^{2-} + H^+) yields a Δ_rG^t of ~17 kJ/mole, resulting in less than 2% change in the overall Δ_rG^t.

References

1. Patil, M.D.; Grogan, G.; Bommarius, A.; Yun, H. Oxidoreductase-catalyzed synthesis of chiral amines. *ACS Catal.* **2018**, *8*, 10985–11015. [CrossRef]
2. Toogood, H.S.; Scrutton, N.S. New developments in 'ene'-reductase catalysed biological hydrogenations. *Curr. Opin. Chem. Biol.* **2014**, *19*, 107–115. [CrossRef] [PubMed]
3. Cosgrove, S.C.; Brzezniak, A.; France, S.P.; Ramsden, J.I.; Mangas-Sanchez, J.; Montgomery, S.L.; Heath, R.S.; Turner, N.J. Imine reductases, reductive aminases, and amine oxidases for the synthesis of chiral amines: Discovery, characterization, and synthetic applications. In *Enzymes in Synthetic Biology*; Scrutton, N., Ed.; Elsevier Academic Press Inc.: San Diego, CA, USA, 2018; Volume 608, pp. 131–149.
4. Bai, D.Y.; He, J.Y.; Ouyang, B.; Huang, J.; Wang, P. Biocatalytic asymmetric synthesis of chiral aryl alcohols. *Prog. Chem.* **2017**, *29*, 491–501.
5. Taylor, M.; Scott, C.; Grogan, G. F-420-dependent enzymes-potential for applications in biotechnology. *Trends Biotechnol.* **2013**, *31*, 63–64. [CrossRef]
6. Mathew, S.; Trajkovic, M.; Kumar, H.; Nguyen, Q.-T.; Fraaije, M.W. Enantio- and regioselective *ene*-reductions using $F_{420}H_2$-dependent enzymes. *Chem. Commun.* **2018**, *54*, 11208–11211. [CrossRef]
7. Greening, C.; Ahmed, F.H.; Mohamed, A.E.; Lee, B.M.; Pandey, G.; Warden, A.C.; Scott, C.; Oakeshott, J.G.; Taylor, M.C.; Jackson, C.J. Physiology, biochemistry, and applications of F_{420}- and Fo-dependent redox reactions. *Microbiol. Mol. Biol. Rev.* **2016**, *80*, 451–493. [CrossRef]
8. Tzing, S.F.; Bryant, M.P.; Wolfe, R.S. Factor 420-dependent pyridine nucleotide-linked formate metabolism of *Methanobacterium ruminantium*. *J. Bacteriol.* **1975**, *121*, 192–196.
9. Eirich, L.D.; Vogels, G.D.; Wolfe, R.S. Distribution of coenzyme F_{420} and properties of its hydrolytic fragments. *J. Bacteriol.* **1979**, *140*, 20–27.
10. Wang, P.; Bashiri, G.; Gao, X.; Sawaya, M.R.; Tang, Y. Uncovering the enzymes that catalyze the final steps in oxytetracycline biosynthesis. *J. Am. Chem. Soc.* **2013**, *135*, 7138–7141. [CrossRef]
11. Li, W.; Chou, S.C.; Khullar, A.; Gerratana, B. Cloning and characterization of the biosynthetic gene cluster for tomaymycin, an SJG-136 monomeric analog. *Appl. Environ. Microbiol.* **2009**, *75*, 2958–2963. [CrossRef]
12. Ahmed, F.H.; Carr, P.D.; Lee, B.M.; Afriat-Jurnou, L.; Mohamed, A.E.; Hong, N.-S.; Flanagan, J.; Taylor, M.C.; Greening, C.; Jackson, C.J. Sequence–structure–function classification of a catalytically diverse oxidoreductase superfamily in *mycobacteria*. *J. Mol. Biol.* **2015**, *427*, 3554–3571. [CrossRef] [PubMed]
13. Selengut, J.D.; Haft, D.H. Unexpected abundance of coenzyme F_{420}-dependent enzymes in *Mycobacterium tuberculosis* and other actinobacteria. *J. Bacteriol.* **2010**, *192*, 5788–5798. [CrossRef] [PubMed]

14. Lapalikar, G.V.; Taylor, M.C.; Warden, A.C.; Onagi, H.; Hennessy, J.E.; Mulder, R.J.; Scott, C.; Brown, S.E.; Russell, R.J.; Easton, C.J.; et al. Cofactor promiscuity among F_{420}-dependent reductases enables them to catalyse both oxidation and reduction of the same substrate. *Catal. Sci. Technol.* **2012**, *2*, 1560–1567. [CrossRef]
15. Harold, L.K.; Antoney, J.; Ahmed, F.H.; Hards, K.; Carr, P.D.; Rapson, T.; Greening, C.; Jackson, C.J.; Cook, G.M. FAD-sequestering proteins protect Mycobacteria against hypoxic and oxidative stress. *J. Biol. Chem.* **2019**, *294*, 2903–2912. [CrossRef] [PubMed]
16. Ahmed, F.H.; Mohamed, A.E.; Carr, P.D.; Lee, B.M.; Condic-Jurkic, K.; O'Mara, M.L.; Jackson, C.J. Rv2074 is a novel $F_{420}H_2$-dependent biliverdin reductase in *Mycobacterium tuberculosis*. *Protein Sci.* **2016**, *25*, 1692–1709. [CrossRef] [PubMed]
17. Mashalidis, E.H.; Mukherjee, T.; Śledź, P.; Matak-Vinković, D.; Boshoff, H.I.; Abell, C.; Barry, C.E. Rv2607 from *Mycobacterium tuberculosis* is a pyridoxine 5′-phosphate oxidase with unusual substrate specificity. *PLoS ONE* **2011**, *6*, e27643. [CrossRef] [PubMed]
18. Taylor, M.C.; Jackson, C.J.; Tattersall, D.B.; French, N.; Peat, T.S.; Newman, J.; Briggs, L.J.; Lapalikar, G.V.; Campbell, P.M.; Scott, C.; et al. Identification and characterization of two families of $F_{420}H_2$-dependent reductases from *Mycobacteria* that catalyse aflatoxin degradation. *Mol. Microbiol.* **2010**, *78*, 561–575. [CrossRef]
19. Cellitti, S.E.; Shaffer, J.; Jones, D.H.; Mukherjee, T.; Gurumurthy, M.; Bursulaya, B.; Boshoff, H.I.; Choi, I.; Nayyar, A.; Lee, Y.S.; et al. Structure of DDN, the deazaflavin-dependent nitroreductase from *Mycobacterium tuberculosis* involved in bioreductive activation of PA-824. *Structure* **2012**, *20*, 101–112. [CrossRef]
20. De Souza, G.A.; Leversen, N.A.; Målen, H.; Wiker, H.G. Bacterial proteins with cleaved or uncleaved signal peptides of the general secretory pathway. *J. Proteom.* **2011**, *75*, 502–510. [CrossRef]
21. He, Z.; De Buck, J. Cell wall proteome analysis of *Mycobacterium smegmatis* strain mc2 155. *BMC Microbiol.* **2010**, *10*, 121. [CrossRef]
22. Sinha, S.; Kosalai, K.; Arora, S.; Namane, A.; Sharma, P.; Gaikwad, A.N.; Brodin, P.; Cole, S.T. Immunogenic membrane-associated proteins of *Mycobacterium tuberculosis* revealed by proteomics. *Microbiology* **2005**, *151*, 2411–2419. [CrossRef] [PubMed]
23. Aufhammer, S.W.; Warkentin, E.; Ermler, U.; Hagemeier, C.H.; Thauer, R.K.; Shima, S. Crystal structure of methylenetetrahydromethanopterin reductase (MER) in complex with coenzyme F_{420}: Architecture of the F_{420}/FMN binding site of enzymes within the nonprolyl *cis*-peptide containing bacterial luciferase family. *Protein Sci.* **2005**, *14*, 1840–1849. [CrossRef] [PubMed]
24. Aufhammer, S.W.; Warkentin, E.; Berk, H.; Shima, S.; Thauer, R.K.; Ermler, U. Coenzyme binding in F_{420}-dependent secondary alcohol dehydrogenase, a member of the bacterial luciferase family. *Structure* **2004**, *12*, 361–370. [CrossRef] [PubMed]
25. Bashiri, G.; Squire, C.J.; Moreland, N.J.; Baker, E.N. Crystal structures of F_{420}-dependent glucose-6-phosphate dehydrogenase FGD1 involved in the activation of the anti-tuberculosis drug candidate PA-824 reveal the basis of coenzyme and substrate binding. *J. Biol. Chem.* **2008**, *283*, 17531–17541. [CrossRef] [PubMed]
26. Nguyen, Q.T.; Trinco, G.; Binda, C.; Mattevi, A.; Fraaije, M.W. Discovery and characterization of an F_{420}-dependent glucose-6-phosphate dehydrogenase (Rh-FGD1) from *rhodococcus jostii* rha1. *Appl. Microbiol. Biotechnol.* **2017**, *101*, 2831–2842. [CrossRef] [PubMed]
27. Mascotti, M.L.; Kumar, H.; Nguyen, Q.-T.; Ayub, M.J.; Fraaije, M.W. Reconstructing the evolutionary history of F_{420}-dependent dehydrogenases. *Sci. Rep.* **2018**, *8*, 17571. [CrossRef] [PubMed]
28. Ceh, K.; Demmer, U.; Warkentin, E.; Moll, J.; Thauer, R.K.; Shima, S.; Ermler, U. Structural basis of the hydride transfer mechanism in F_{420}-dependent methylenetetrahydromethanopterin dehydrogenase. *Biochemistry* **2009**, *48*, 10098–10105. [CrossRef]
29. Shima, S.; Warkentin, E.; Grabarse, W.; Sordel, M.; Wicke, M.; Thauer, R.K.; Ermler, U. Structure of coenzyme F_{420} dependent methylenetetrahydromethanopterin reductase from two methanogenic archaea. *J. Mol. Biol.* **2000**, *300*, 935–950. [CrossRef]
30. Vaupel, M.; Thauer, R.K. Coenzyme F_{420} dependent N-5, N-10-methylenetetrahydromethanopterin reductase (MER) from *Methanobacterium thermautotrophicum* strain marburg: Cloning, sequencing, transcriptional analysis and functional expression in *Escherichia coli* of the *mer* gene. *Eur. J. Biochem.* **1995**, *231*, 773–778.
31. Purwantini, E.; Mukhopadhyay, B. Rv0132c of *Mycobacterium tuberculosis* encodes a coenzyme F_{420}-dependent hydroxymycolic acid dehydrogenase. *PLoS ONE* **2013**, *8*, e81985. [CrossRef]

32. Fida, T.T.; Palamuru, S.; Pandey, G.; Spain, J.C. Aerobic biodegradation of 2,4-dinitroanisole by *Nocardioides* sp. Strain js1661. *Appl. Environ. Microbiol.* **2014**, *80*, 7725–7731. [CrossRef] [PubMed]
33. Ebert, S.; Rieger, P.G.; Knackmuss, H.J. Function of coenzyme f_{420} in aerobic catabolism of 2,4,6-trinitrophenol and 2,4-dinitrophenol by *Nocardioides simplex* FJ2-1A. *J. Bacteriol.* **1999**, *181*, 2669–2674. [PubMed]
34. Lapalikar, G.V.; Taylor, M.C.; Warden, A.C.; Scott, C.; Russell, R.J.; Oakeshott, J.G. $F_{420}H_2$-dependent degradation of aflatoxin and other furanocoumarins is widespread throughout the *Actinomycetales*. *PLoS ONE* **2012**, *7*, e30114. [CrossRef] [PubMed]
35. Greening, C.; Jirapanjawat, T.; Afroze, S.; Ney, B.; Scott, C.; Pandey, G.; Lee, B.M.; Russell, R.J.; Jackson, C.J.; Oakeshott, J.G.; et al. Mycobacterial $F_{420}H_2$-dependent reductases promiscuously reduce diverse compounds through a common mechanism. *Front. Microbiol.* **2017**, *8*. [CrossRef]
36. Gurumurthy, M.; Rao, M.; Mukherjee, T.; Rao, S.P.S.; Boshoff, H.I.; Dick, T.; Barry, C.E.; Manjunatha, U.H. A novel F_{420}-dependent anti-oxidant mechanism protects *Mycobacterium tuberculosis* against oxidative stress and bactericidal agents. *Mol. Microbiol.* **2013**, *87*, 744–755. [CrossRef]
37. Mohamed, A.E.; Ahmed, F.H.; Arulmozhiraja, S.; Lin, C.Y.; Taylor, M.C.; Krausz, E.R.; Jackson, C.J.; Coote, M.L. Protonation state of $F_{420}H_2$ in the prodrug-activating deazaflavin dependent nitroreductase (DDN) from *Mycobacterium tuberculosis*. *Mol. BioSys.* **2016**, *12*, 1110–1113. [CrossRef]
38. Drenth, J.; Trajkovic, M.; Fraaije, M.W. Chemoenzymatic synthesis of an unnatural deazaflavin cofactor that can fuel F_{420}-dependent enzymes. *ACS Catal.* **2019**, *9*, 6435–6443. [CrossRef]
39. Purwantini, E.; Daniels, L. Molecular analysis of the gene encoding F_{420}-dependent glucose-6-phosphate dehydrogenase from *Mycobacterium smegmatis*. *J. Bacteriol.* **1998**, *180*, 2212–2219.
40. Bleicher, K.; Winter, J. Purification and properties of F_{420}-and $NADP^+$-dependent alcohol dehydrogenases of *Methanogenium liminatans* and *Methanobacterium palustre*, specific for secondary alcohols. *Europ. J. Biochem.* **1991**, *200*, 43–51. [CrossRef]
41. Knaus, T.; Cariati, L.; Masman, M.F.; Mutti, F.G. In vitro biocatalytic pathway design: Orthogonal network for the quantitative and stereospecific amination of alcohols. *Org. Biomol. Chem.* **2017**, *15*, 8313–8325.
42. Guo, F.; Berglund, P. Transaminase biocatalysis: Optimization and application. *Green Chem.* **2017**, *19*, 333–360. [CrossRef]
43. Adams, J.P.; Brown, M.J.B.; Diaz-Rodriguez, A.; Lloyd, R.C.; Roiban, G.D. Biocatalysis: A pharma perspective. *Adv. Synth. Catal.* **2019**, *361*, 2421–2432. [CrossRef]
44. Musa, M.M.; Hollmann, F.; Mutti, F.G. Synthesis of enantiomerically pure alcohols and amines *via* biocatalytic deracemisation methods. *Cat. Sci. Technol.* **2019**, *9*, 10–1039. [CrossRef]
45. Ichikawa, H.; Bashiri, G.; Kelly, W.L. Biosynthesis of the thiopeptins and identification of an $F_{420}H_2$-dependent dehydropiperidine reductase. *J. Am. Chem. Soc.* **2018**, *140*, 10749–10756. [CrossRef]
46. Miller, A.F.; Park, J.T.; Ferguson, K.L.; Pitsawong, W.; Bommarius, A.S. Informing efforts to develop nitroreductase for amine production. *Molecules* **2018**, *23*, 22. [CrossRef]
47. Heiss, G.; Hofmann, K.W.; Trachtmann, N.; Walters, D.M.; Rouvière, P.; Knackmuss, H.J. *Npd* gene functions of *Rhodococcus (opacus) erythropolis* Hl PM-1 in the initial steps of 2,4,6-trinitrophenol degradation. *Microbiology* **2002**, *148*, 799–806. [CrossRef]
48. Xu, J.; Green, A.P.; Turner, N.J. Chemo-enzymatic synthesis of pyrazines and pyrroles. *Angew. Chem.-Int. Ed.* **2018**, *57*, 16760–16763. [CrossRef]
49. Busacca, C.A.; Fandrick, D.R.; Song, J.J.; Senanayake, C.H. The growing impact of catalysis in the pharmaceutical industry. *Adv. Synth. Catal.* **2011**, *353*, 1825–1864. [CrossRef]
50. Heiss, G.; Trachtmann, N.; Abe, Y.; Takeo, M.; Knackmuss, H.J. Homologous *npdgi* genes in 2,4-dinitrophenol- and 4-nitrophenol-degrading *Rhodococcus* spp. *Appl. Environ. Microbiol.* **2003**, *69*, 2748–2754. [CrossRef]
51. Purwantini, E.; Daniels, L.; Mukhopadhyay, B. $F_{420}H_2$ is required for phthiocerol dimycocerosate synthesis in *Mycobacteria*. *J. Bacteriol.* **2016**, *198*, 2020–2028. [CrossRef]
52. Wichmann, R.; Vasic-Racki, D. Cofactor regeneration at the lab scale. In *Technology Transfer in Biotechnology*; Springer: Berlin, Germany, 2005; pp. 225–260.
53. Tishkov, V.I.; Popov, V.O. Catalytic mechanism and application of formate dehydrogenase. *Biochemistry* **2004**, *69*, 1252. [CrossRef] [PubMed]
54. Eguchi, T.; Kuge, Y.; Inoue, K.; Yoshikawa, N.; Mochida, K.; Uwajima, T. NADPH regeneration by glucose dehydrogenase from *Gluconobacter scleroides* for L-leucovorin synthesis. *Biosci. Biotechnol. Biochem.* **1992**, *56*, 701–703. [CrossRef] [PubMed]

55. Demir, A.S.; Talpur, F.N.; Sopaci, B.; Kohring, G.-W.; Celik, A. Selective oxidation and reduction reactions with cofactor regeneration mediated by galactitol-, lactate-, and formate dehydrogenases immobilized on magnetic nanoparticles. *J. Biotechnol.* **2011**, *152*, 176–183. [CrossRef] [PubMed]
56. Wong, C.-H.; Whitesides, G.M. Enzyme-catalyzed organic synthesis: NAD(P)H cofactor regeneration by using glucose-6-phosphate and the glucose-5-phosphate dehydrogenase from *Leuconostoc mesenteroides*. *J. Am. Chem. Soc.* **1981**, *103*, 4890–4899. [CrossRef]
57. Lee, W.-H.; Park, J.-B.; Park, K.; Kim, M.-D.; Seo, J.-H. Enhanced production of ϵ-caprolactone by overexpression of NADPH-regenerating glucose 6-phosphate dehydrogenase in recombinant *Escherichia coli* harboring cyclohexanone monooxygenase gene. *Appl. Microbiol. Biotechnol.* **2007**, *76*, 329–338. [CrossRef] [PubMed]
58. Berrios-Rivera, S.J.; Bennett, G.N.; San, K.Y. Metabolic engineering of *Escherichia coli*: Increase of NADH availability by overexpressing an NAD^+-dependent formate dehydrogenase. *Metab. Eng.* **2002**, *4*, 217–229. [CrossRef]
59. Bashiri, G.; Antoney, J.; Jirgis, E.N.M.; Shah, M.V.; Ney, B.; Copp, J.; Stuteley, S.M.; Sreebhavan, S.; Palmer, B.; Middleditch, M.; et al. A revised biosynthetic pathway for the cofactor F_{420} in prokaryotes. *Nat. Commun.* **2019**, *10*, 1558. [CrossRef]
60. Purwantini, E.; Daniels, L. Purification of a novel coenzyme F_{420}-dependent glucose-6-phosphate dehydrogenase from *Mycobacterium smegmatis*. *J. Bacteriol.* **1996**, *178*, 2861–2866. [CrossRef]
61. Costa, K.C.; Wong, P.M.; Wang, T.; Lie, T.J.; Dodsworth, J.A.; Swanson, I.; Burn, J.A.; Hackett, M.; Leigh, J.A. Protein complexing in a methanogen suggests electron bifurcation and electron delivery from formate to heterodisulfide reductase. *Proc. Natl. Acad. Sci. USA* **2010**, *107*, 11050–11055. [CrossRef]
62. Shuber, A.P.; Orr, E.C.; Recny, M.A.; Schendel, P.F.; May, H.D.; Schauer, N.L.; Ferry, J.G. Cloning, expression, and nucleotide sequence of the formate dehydrogenase genes from *Methanobacterium formicicum*. *J. Biol. Chem.* **1986**, *261*, 12942–12947.
63. Novotná, J.; Neužil, J.; Hoš?álek, Z. Spectrophotometric identification of 8-hydroxy-5-deazaflavin: Nadph oxidoreductase activity in *Streptomycetes* producing tetracyclines. *FEMS Microbiol. Lett.* **1989**, *59*, 241–245. [CrossRef]
64. Kumar, H.; Nguyen, Q.T.; Binda, C.; Mattevi, A.; Fraaije, M.W. Isolation and characterization of a thermostable F_{420}:NADPH oxidoreductase from *Thermobifida fusca*. *J. Biol. Chem.* **2017**, *292*, 10123–10130. [CrossRef] [PubMed]
65. Kunow, J.; Schwörer, B.; Stetter, K.O.; Thauer, R.K. A F_{420}-dependent NADP reductase in the extremely thermophilic sulfate-reducing *Archaeoglobus fulgidus*. *Arch. Microbiol.* **1993**, *160*, 199–205.
66. Eker, A.P.M.; Hessels, J.K.C.; Meerwaldt, R. Characterization of an 8-hydroxy-5-deazaflavin: NADPH oxidoreductase from *Streptomyces griseus*. *Biochim. Biophys. Acta* **1989**, *990*, 80–86. [CrossRef]
67. Seelbach, K.; Riebel, B.; Hummel, W.; Kula, M.R.; Tishkov, V.I.; Egorov, A.M.; Wandrey, C.; Kragl, U. A novel, efficient regenerating method of NADPH using a new formate dehydrogenase. *Tetrahedron Lett.* **1996**, *37*, 1377–1380. [CrossRef]
68. Alex, L.A.; Reeve, J.N.; Ormejohnson, W.H.; Walsh, C.T. Cloning, sequence determination, and expression of the genes encoding the subunits of the nickel-containing 8-hydroxy-5-deazaflavin reducing hydrogenase from *Methanobacterium thermoautotrophicum* delta-H. *Biochemistry* **1990**, *29*, 7237–7244. [CrossRef]
69. Tersteegen, A.; Hedderich, R. *Methanobacterium thermoautotrophicum* encodes two multisubunit membrane-bound NiFe hydrogenases - transcription of the operons and sequence analysis of the deduced proteins. *Eur. J. Biochem.* **1999**, *264*, 930–943. [CrossRef]
70. Hocking, W.P.; Stokke, R.; Roalkvam, I.; Steen, I.H. Identification of key components in the energy metabolism of the hyperthermophilic sulfate-reducing archaeon *archaeoglobus fulgidus* by transcriptome analyses. *Front. Microbiol.* **2014**, *5*, 20. [CrossRef]
71. Vitt, S.; Ma, K.; Warkentin, E.; Moll, J.; Pierik, A.J.; Shima, S.; Ermler, U. The F-420-reducing NiFe -hydrogenase complex from *methanothermobacter marburgensis*, the first x-ray structure of a group 3 family member. *J. Mol. Biol.* **2014**, *426*, 2813–2826. [CrossRef]
72. Bashiri, G.; Rehan, A.M.; Greenwood, D.R.; Dickson, J.M.; Baker, E.N. Metabolic engineering of cofactor F_{420} production in *Mycobacterium smegmatis*. *PLoS ONE* **2010**, *5*, e15803. [CrossRef]
73. Isabelle, D.; Simpson, D.R.; Daniels, L. Large-scale production of coenzyme F_{420}-5,6 by using *Mycobacterium smegmatis*. *Appl. Environ. Microbiol.* **2002**, *68*, 5750–5755. [CrossRef] [PubMed]

74. Eker, A.P.M.; Pol, A.; van der Meyden, P.; Vogels, G.D. Purification and properties of 8-hydroxy-5-deazaflavin derivatives from *Streptomyces griseus*. *FEMS Microbiol. Lett.* **1980**, *8*, 161–165. [CrossRef]
75. Grochowski, L.L.; Xu, H.M.; White, R.H. Identification and characterization of the 2-phospho-L-lactate guanylyltransferase involved in coenzyme F-420 biosynthesis. *Biochemistry* **2008**, *47*, 3033–3037. [CrossRef] [PubMed]
76. Braga, D.; Lasta, D.; Hasan, M.; Guo, H.; Leichnitz, D.; Uzum, Z.; Richter, I.; Schalk, F.; Beemelmanns, C.; Hertweck, C.; et al. Metabolic pathway rerouting in *Paraburkholderia rhizoxinica* evolved long-overlooked derivatives of coenzyme F_{420}. *ACS Chem. Biol.* **2019**, 2088–2094. [CrossRef]
77. Hossain, M.S.; Le, C.Q.; Joseph, E.; Nguyen, T.Q.; Johnson-Winters, K.; Foss, F.W. Convenient synthesis of deazaflavin cofactor F_o and its activity in F_{420}-dependent NADP reductase. *Organ. Biomol. Chem.* **2015**, *13*, 5082–5085. [CrossRef]
78. Alberty, R.A. Calculation of standard transformed formation properties of biochemical reactants and standard apparent reduction potentials of half reactions. *Arch. Biochem. Biophys.* **1998**, *358*, 25–39. [CrossRef]
79. Alberty, R.A. Calculation of standard transformed gibbs energies and standard transformed enthalpies of biochemical reactants. *Arch. Biochem. Biophys.* **1998**, *353*, 116–130. [CrossRef]
80. Benedict, M.N.; Gonnerman, M.C.; Metcalf, W.W.; Price, N.D. Genome-scale metabolic reconstruction and hypothesis testing in the methanogenic archaeon *Methanosarcina acetivorans* C2A. *J. Bacteriol.* **2012**, *194*, 855–865. [CrossRef]
81. Jankowski, M.D.; Henry, C.S.; Broadbelt, L.J.; Hatzimanikatis, V. Group contribution method for thermodynamic analysis of complex metabolic networks. *Biophys. J.* **2008**, *95*, 1487–1499. [CrossRef]
82. Henry, C.S.; DeJongh, M.; Best, A.A.; Frybarger, P.M.; Linsay, B.; Stevens, R.L. High-throughput generation, optimization and analysis of genome-scale metabolic models. *Nat. Biotechnol.* **2010**, *28*, 977–982. [CrossRef]
83. Nazem-Bokaee, H.; Gopalakrishnan, S.; Ferry, J.G.; Wood, T.K.; Maranas, C.D. Assessing methanotrophy and carbon fixation for biofuel production by *Methanosarcina acetivorans*. *Microb. Cell Fact.* **2016**, *15*, 10. [CrossRef] [PubMed]
84. Caspi, R.; Billington, R.; Fulcher, C.A.; Keseler, I.M.; Kothari, A.; Krummenacker, M.; Latendresse, M.; Midford, P.E.; Ong, Q.; Ong, W.K.; et al. The metacyc database of metabolic pathways and enzymes. *Nucleic Acids Res.* **2018**, *46*, D633–D639. [CrossRef] [PubMed]